1521-009X/12/4003-625–634$25.00
DRUG METABOLISM AND DISPOSITION

DMD 40:625–634, 2012

Vol. 40, No. 3
42770/3752997

DRUG METABOLISM & DISPOSITION

Deuterium Isotope Effects on Drug Pharmacokinetics. I. System-Dependent Effects of Specific Deuteration with Aldehyde Oxidase Cleared Drugs

Raman Sharma, Timothy J. Strelevitz, Hongying Gao, Alan J. Clark, Klaas Schildknegt, R. Scott Obach, Sharon L. Ripp, Douglas K. Spracklin, Larry M. Tremaine, and Alfin D. N. Vaz

Departments of Pharmacokinetics Dynamics and Metabolism (R.S., T.J.S., H.G., A.J.C., R.S.O., S.L.R., D.K.S., L.M.T., A.D.N.V.) and Pharmaceutical Sciences (K.S.), Pfizer Global Research and Development, Groton, Connecticut

Received September 14, 2011; accepted December 15, 2011

ABSTRACT:

The pharmacokinetic properties of drugs may be altered by kinetic deuterium isotope effects. With specifically deuterated model substrates and drugs metabolized by aldehyde oxidase, we demonstrate how knowledge of the enzyme's reaction mechanism, species differences in the role played by other enzymes in a drug's metabolic clearance, and differences in systemic clearance mechanisms are critically important for the pharmacokinetic application of deuterium isotope effects. Ex vivo methods to project the in vivo outcome using deuterated carbazeran and zoniporide with hepatic systems demonstrate the importance of establishing the extent to which other metabolic enzymes contribute to the metabolic clearance mechanism. Differences in pharmacokinetic outcomes in guinea pig and rat, with the same metabolic clearance mechanism, show how species differences in the systemic clearance mechanism can affect the in vivo outcome. Overall, to gain from the application of deuteration as a strategy to alter drug pharmacokinetics, these studies demonstrate the importance of understanding the systemic clearance mechanism and knowing the identity of the metabolic enzymes involved, the extent to which they contribute to metabolic clearance, and the extent to which metabolism contributes to the systemic clearance.

Introduction

Deuteration of drugs to enhance their pharmacokinetic, pharmacodynamic, or toxicological properties has gained momentum as judged by a search of the SciFinder database with the search term "deuterated drugs." Of 179 registries retrieved, 151 are since 2005 with an exponential growth since 2006. These include deuterated versions of patented and off-patent drugs with claims of increased efficacy, decreased toxicity, reduced interpatient variability, and decreased drug dose or dosing frequency. Belleau et al. (1961) were among the first to demonstrate the pharmacodynamic effect of deuteration with $\alpha\alpha$-dideuterated *p*-tyramine. The effect was attributed to decreased metabolism of *p*-tyramine by monoamine oxidases. Several reports that have examined the effect of deuteration on the pharmacokinetic and pharmacodynamic properties of drugs reveal results that include little to no effect (Tanabe et al., 1970; Farmer et al., 1979; Taylor et al., 1983; Burm et al., 1988; Dunsaed et al., 1995); increased systemic exposure, a pharmacodynamic effect, and receptor selectivity (Dyck et al., 1988; Schneider et al., 2006, 2007); and decreased toxicity (Najjar et al., 1978). However, in these studies the mechanisms underlying the observed effects or lack thereof were not examined. With the use of formyl-deuterated *N*-methylformamide, the hepatotoxicity was shown to be due to oxidative metabolism at the formyl carbon (Threadgill et al., 1989). Pohl and Gillette (1984–1985) outlined the kinetic basis for use of deuterated compounds to determine toxic metabolic pathways, and, in addition, Nelson and Trager (2003) have reviewed distinctions between "intrinsic KDIEs" and "observed KDIEs" in enzyme reaction mechanisms with particular emphasis on cytochrome P450 reactions. Foster (1984) and Kushner et al. (1999) have also discussed the application of deuterated drugs to drug pharmacokinetics, pharmacodynamics, and toxicity.

A KDIE on the intrinsic metabolic clearance (CL_{int} or V_{max}/K_m) is fundamental to the application of a deuteration strategy to alter drug pharmacokinetics. Multiple factors mute the magnitude of this isotope effect. These include substantial contribution to the metabolic clearance by conjugating enzymes (UDP-glucuronosyltransferases, sulfotransferases, and glutathione transferases) and heteroatom oxidizing enzymes (flavin monooxygenases), in which carbon-hydrogen bonds are not broken; aspects of enzyme reaction mechanisms such as "metabolic switching" due to deuterium substitution, particularly important with cytochrome P450 cleared molecules (Miwa and Lu, 1987; Nelson and Trager, 2003); rate-limiting product release from enzymes, which mask intrinsic KDIEs (Ling and Hanzlik, 1989; Hall and Hanzlik, 1990; Bell-Parikh and Guengerich, 1999); and other biological processes such as organ blood flow-limited clearance, renal and/or biliary clearance by passive or active transport involving uptake or efflux pumps and enterohepatic recycling. Consequently, a

Article, publication date, and citation information can be found at http://dmd.aspetjournals.org.
http://dx.doi.org/10.1124/dmd.111.042770.

ABBREVIATIONS: KDIE, kinetic deuterium isotope effect; LC, liquid chromatography; MS, mass spectrometry; QC, quality control; MRM, multiple reaction monitoring; AO, aldehyde oxidase; AUC, area under the curve.

KDIE on the intrinsic metabolic clearance alone may not translate into an alteration of the overall pharmacokinetics of a drug.

Drug design strategies have successfully decreased the impact of cytochrome P450 enzymes in metabolic clearance, partly by increased use of nitrogen heteroaromatics in drug substructures. As a consequence, aldehyde oxidase is increasingly observed as an alternate metabolic pathway for clearance because of its ability to oxidize nitrogen heteroaromatic ring systems. The broad differential tissue distribution of this enzyme results in an inability to correlate in vitro intrinsic clearance to in vivo clearance, and failure of allometric scaling of clearance due to interspecies differences in this enzyme have resulted in design strategies to avoid its role in metabolic clearance (Pryde et al., 2010). An alternate approach to decrease clearance when this enzyme is involved may be the use of KDIEs with specifically deuterated substrates.

In this study, we focused on aldehyde oxidase as the metabolic clearance enzyme using specifically deuterated substrates to establish mechanistic consistency across species and two Pfizer drugs, carbazeran and zoniporide, for which some preclinical and clinical information was available, to demonstrate the importance of knowing the enzyme(s) involved in the metabolic clearance, their reaction mechanisms, the species differences in metabolic pathways, and the use of in vitro methods to assess the probability for in vivo success. We have determined 1) in vitro intra- and intermolecular KDIEs for several aldehyde oxidase substrates, 2) in vitro KDIE on the intrinsic clearances and metabolic profiles in hepatocytes and hepatic subcellular fractions, and 3) the in vivo KDIEs on pharmacokinetic parameters for carbazeran and zoniporide administered orally and intravenously. Carbazeran was a phosphodiesterase-2 inhibitor for the treatment of chronic heart failure, discontinued because of low oral bioavailability (<5%) and short half-life in humans (Kaye et al., 1984), and zoniporide was a Na^+/H^+ exchanger-1 inhibitor for treatment of perioperative myocardial ischemic injury after surgery, for which high clearance was observed in humans and rats (Dalvie et al., 2010).

Materials and Methods

Unless otherwise stated, all reagents used in chemical syntheses and biochemical and biological studies were of reagent grade and used as such without further purification.

Deuterated Substrates. Scheme 1 shows the synthetic approaches used to deuterate the substrates used in this study. The palladium-catalyzed reductive deuteration of α-chloro-heterocycles and the base-catalyzed deuterium exchange of the α-hydrogen in heterocycle-*N*-oxides are well established methods for the specific introduction of deuterium into selected sites of nitrogen heterocycles (Kawazoe and Onishi, 1967; Rylander, 1985).

2-[^{2}H]Quinoxaline, 1-[^{2}H]phthalazine, and 2-[^{2}H]quinoline. These were synthesized from their corresponding chloro derivatives by palladium-catalyzed reduction (Scheme 1a) (Rylander, 1985) and described for 2-[^{2}H]quinoxaline. A solution of 2-chloroquinoxaline (0.30 g, 1.82 mmol) in 10 ml of EtOD and 0.3 ml of tetraethylammonium was purged with N_2 gas, and 20 mg of 20% $Pd(OH)_2/C$ was added. The suspension was then purged with D_2 (>99% isotopic purity) gas followed by stirring at room temperature for 4 h under a balloon of D_2 gas. Before filtering, the reaction was purged with N_2 gas, and the filtrate was concentrated under reduced pressure. The residue was dissolved in 30 ml of EtOAc, washed with 30 ml of H_2O, and concentrated under reduced pressure. Flash column chromatography of the residue on an ISCO silica gel cartridge eluting with 20% EtOAc/80% hexanes afforded 23 mg (10% yield) of quinoxaline-*d* as an off-white solid. LC-MS: *m/z* 132 (MH^+); monodeuterium isotopic content >99%.

1-[^{2}H]Carbazeran. 1-[^{2}H]carbazeran (CAS Registry Number 70724-25-3) was synthesized as shown in Scheme 1b. A solution of 1,4-dichloro-6,7-dimethoxyphthalazine **b1** (500 mg, 1.93 mmol) in 5 ml of dimethylformamide was treated with piperidine **b2** (432 mg, 1.93 mmol, 1.3 Eq), K_2CO_3 (800 mg, 5.79 mmol, 3 Eq), and KI (20 mg, 0.12 mmol, 0.06 Eq). The resulting suspension was heated at 110°C for 4 h and then cooled to room temperature. The reaction was diluted with 20 ml of H_2O and extracted with 20 ml of EtOAc. The EtOAc layer was washed two times with 10 ml of brine, dried over anhydrous Na_2SO_4, and concentrated under reduced pressure to afford 680 mg (89% yield) of **b3** as a white solid. A suspension of **b3** (500 mg, 1.27 mmol) in 35 ml of EtOD and 2 ml of tetraethylammonium was purged with N_2 gas. To the suspension was added 30 mg of 10% Pd/C, and after purging with D_2 gas the reaction was stirred under a balloon of D_2 gas for 3 h at room temperature. The reaction was then purged with N_2 gas and filtered, and the filtrate was concentrated under reduced pressure. The residue was dissolved in 30 ml of EtOAc, washed with 30 ml of H_2O followed by 10 ml of brine, and dried over Na_2SO_4. The solvent was evaporated under reduced pressure, and the resulting residue was purified by flash column chromatography (ISCO silica gel cartridge eluting with 100% CH_2Cl_2 to 90% CH_2Cl_2/10% MeOH) to afford 360 mg (79% yield) of 1-[^{2}H]carbazeran as a tan solid. LC-MS: *m/z* 362 (MH^+); monodeuterium isotopic content >99%.

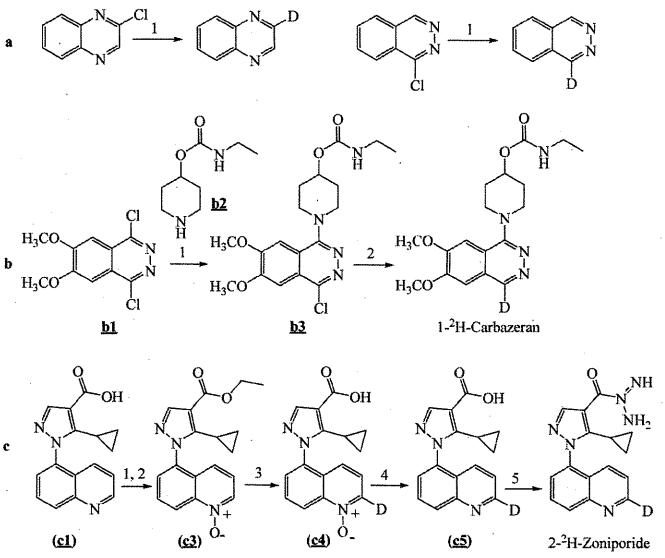

SCHEME 1. Sequence of synthetic steps used to deuterate compounds used in this study.

2-[^{2}H]Zoniporide. 2-[^{2}H]zoniporide (CAS Registry Number 241800-98-6) was synthesized as shown in Scheme 1c. A suspension of quinoline carboxylic acid (**c1**, 4.00 g, 14.32 mmol) in 70 ml of EtOH and 1 ml of H_2SO_4 was heated at reflux for 18 h. An additional 1.5 ml of H_2SO_4 was added to the reaction, and reflux was continued for 20 h. The resulting reaction solution was cooled to room temperature and concentrated to approximately one-third of its volume by rotary evaporation. The residual solution was diluted with 150 ml of Et_2O and washed two times with 50 ml of saturated aqueous $NaHCO_3$ followed by 50 ml of brine. The organic layer was dried over Na_2SO_4 and concentrated under reduced pressure to afford 3.85 g (88% yield) of the ethyl ester as a brown oil. The ester (2.35 g, 7.65 mmol) and 3-chloroperoxybenzoic acid (2.32 g; 13.44 mmol, 1.8 Eq) in 70 ml of $CHCl_3$ were stirred at room temperature for 16 h. The reaction solution was diluted with 30 ml of $CHCl_3$ and washed with 50 ml of saturated aqueous $NaHCO_3$, 50 ml of saturated aqueous $NaHSO_3$, and finally 50 ml of brine. The organic layer was dried over Na_2SO_4 and concentrated under reduced pressure to afford 2.74 g of crude **c3** as a light brown oil.

A suspension of **c3** (3.30 g, 10.21 mmol) in 70 ml of D_2O (99.9% D) was treated with 2 ml of 50% NaOD in D_2O, and the resulting solution was heated at 100°C for 3 h (Kawazoe and Onishi, 1967). The reaction was cooled to room temperature, and the pH of the solution was adjusted to 4.0 by dropwise addition of D_2SO_4. The resulting suspension was extracted three times with 100 ml of $CHCl_3$. The combined organic layers were dried over Na_2SO_4 and concentrated under reduced pressure. The crude product residue was purified by flash column chromatography (ISCO silica gel cartridge eluting with 97.4% CH_2Cl_2/2.5% MeOH/0.1% AcOH to 94.9% CH_2Cl_2/5% MeOH/0.1% AcOH) to afford 2.20 g (73% yield) of **c4** as a light yellow solid. LC-MS: *m/z* 297 (MH^+); monodeuterium isotopic content >98%.

A solution of **c4** (0.72 g, 2.42 mmol) in 18 ml of MeOD was purged with N_2 gas and treated with 126 mg of 10% Pd/C followed by ammonium formate (0.72 g, 11.42 mmol, 4.7 Eq). The resulting suspension was heated at 45°C for 1 h and then cooled to room temperature and filtered. The filtrate was concentrated, and the resulting residue was diluted with 50 ml of H_2O and extracted into 50 ml of $CHCl_3$ containing 0.5 ml of AcOH. The organic layer was dried over Na_2SO_4 and concentrated under reduced pressure to afford 570 mg (84% yield) of **c5** as an off-white solid.

A solution of **c5** (0.35 g, 1.25 mmol) in 8 ml of $SOCl_2$ was heated at reflux for 1 h. The solution was then cooled to room temperature and concentrated to a yellow solid by rotary evaporation. The solid was treated with 5 ml of toluene and again evaporated under reduced pressure to a solid. The solid was then suspended in 9 ml of tetrahydrofuran, and this suspension was added to a solution of guanidine-HCl (0.74 g, 7.75 mmol, 6.2 Eq) in 14 ml of 1 M aqueous NaOH and 7 ml of tetrahydrofuran. The reaction was heated at 45°C for 1 h and then cooled to room temperature to afford a biphasic solution. The organic layer was partially concentrated, and the resulting liquid was extracted with 25 ml of 5:1 $CHCl_3$-isopropyl alcohol. The organic layer was dried over Na_2SO_4 and dried under vacuum. The resulting crude product was slurried in 5 ml of ice-cold EtOAc and filtered to afford 150 mg (38% yield) of 2-[^{2}H]zoniporide as an off-white solid. LC-MS: *m/z* 322.2 (MH^+); monodeuterium isotopic content >98%.

Biological Reagents. Human and rat liver cytosols were purchased from BD Gentest (Woburn, MA). Guinea pig liver S-9 and cytosol were purchased from XenoTech, LLC (Lenexa, KS). Pooled and cryopreserved hepatocytes from either human or rat livers were obtained from Celsis In Vitro Technologies (Baltimore, MD).

Human aldehyde oxidase was partially purified from pooled liver cytosol by ammonium sulfate precipitation as follows. To a liter of stirred human liver cytosol preparation (obtained as a recovery fraction from the preparation of liver microsomes) maintained in an ice-water bath, buffered with 100 mM potassium phosphate buffer, pH 7.4, and constantly monitored for pH, was added solid ammonium sulfate (in small amounts at a time) to four weight to volume cuts of 5, 15, 20, and 25% ammonium sulfate. The pH was constantly adjusted with a 1 M solution of potassium mono-hydrogen phosphate (K_2HPO_4) to maintain it between 7.0 and 7.4. After each weight to volume addition of ammonium sulfate, the suspension was stirred for 30 min to equilibrate, then centrifuged at 9000*g* for 20 min to pellet precipitated protein. The protein pellets were redissolved in 100 ml of 10 mM potassium phosphate buffer, pH 7.4, and assayed for aldehyde oxidase activity, as measured by the oxidation of phenanthridine to phenanthridone. The aldehyde oxidase activity was recovered in the 20 and 25% w/v ammonium sulfate protein pellets. The oxidase activity of this preparation of aldehyde oxidase was stable at −40°C for more than 1 year.

Bioanalytical Procedures. A 1 atomic mass unit difference between the proto and deutero forms of the substrates used in these studies required an accurate correction of the mass spectral contribution from the natural abundance from ^{13}C in the proto forms of the compounds to the base mass of the deutero forms. The difference in the contribution determined empirically from standard curves to that calculated from molecular formulas is less than 1%.

Sample Preparation. All standards, QC samples, and samples were prepared using the Hamilton MicroLab STAR (Reno, NV) robotic sample preparation station. A working solution of 4 μg/ml zoniporide or deuterated zoniporide was prepared separately by diluting 1 mg/ml stock solution in 1:1 dimethyl sulfoxide-acetonitrile. Sequential dilution of the working solution in blank Sprague-Dawley plasma yielded standard solutions of 0.1, 0.2, 0.5, 1, 5, 10, 50, 100, and 200 ng/ml and QC samples of 0.4, 8, and 80 ng/ml in plasma. A working solution of 10 μg/ml carbazeran or deuterated carbazeran was prepared separately by diluting 1 mg/ml stock solution in 1:1 dimethyl sulfoxide-acetonitrile. Sequential dilution of the working solution in blank guinea pig plasma yielded standard solutions of 0.1, 0.2, 0.5, 1, 2, 5, 10, 50, 100, 200, and 500 ng/ml and QC samples of 0.8, 8, 80, and 400 ng/ml in plasma. In the cassette-dosed studies of zoniporide the early time points between 0.16 and 0.75 h were diluted 10- and 5-fold in blank Sprague-Dawley plasma. For the carbazeran cassette-dosed study, samples at time points between 10 and 30 min were diluted 10-fold in blank guinea pig plasma with the exception of the 10-min time point in the intravenous study that was diluted 20-fold. To each 50-μl standard or sample solution from the zoniporide study was added 200 μl of acetonitrile containing 10 ng/ml internal standard for protein precipitation. The solutions were mixed and centrifuged at 3000*g* for 20 min. Then 120 μl of the supernatant from standard and sample mixtures was transferred to a 96-deep well plate and diluted 1:1 with 0.1% formic acid in water. To 120 μl of standard and sample solutions in the carbazeran study was added 480 μl of 0.1% formic acid in 1:1 acetonitrile-water. After mixing, the solutions were analyzed by LC-tandem mass spectrometry as follows. An API 4000 mass spectrometer (Applied Biosystems/MDS Sciex, Foster City, CA) equipped with Turbo V sources and a TurboIonSpray interface integrated with a Prominence LC-AD20 binary pump (Shimadzu, Columbia, MD) and an autosampler (PAL; CTC Analytics AG, Zwingen, Switzerland) with a cool stack temperature controlled at 4–8°C was used for analysis. All instruments were controlled and synchronized by Analyst software from Applied Biosystems/MDS Sciex.

Ten-microliter aliquots of the zoniporide samples were injected onto a C-18 reversed phase column (Luna C18-2, 5-μm, 2.0 × 30 mm; Phenomenex, Torrance, CA) equilibrated with 5% solvent B (0.1% formic acid in acetonitrile) in solvent A (0.1% formic acid in water) and maintained for 0.6 min after injection followed by a linear gradient to 98% solvent B over 0.65 min and held for 0.55 min and then returned to the original conditions in 0.4 min for a cycle time of 3.0 min. The flow rate for the zoniporide analysis was 0.5 ml/min. The column was equilibrated at 5% solvent B for 0.8 min before reinjection. For the analysis of carbazeran, the flow rate was 0.6 ml/min. The gradient was maintained at 5% solvent B for 0.6 min, followed by a linear increase to 98% solvent B in 0.65 min, and kept at 98% solvent B for 0.95 min, followed by a linear decrease to 5% in 0.2 min. The column was equilibrated at 5% B for 0.6 min before reinjection.

The ionization parameters for the compounds were optimized by direct infusion of undiluted standards in 50% aqueous acetonitrile containing 0.1% formic acid. The multiple reaction monitoring (MRM) transitions for carbazeran and 1-[^{2}H]carbazeran were *m/z* 361.2 to *m/z* 272.2 and *m/z* 362.2 to *m/z* 273.2, respectively. For zoniporide and 2-[^{2}H]zoniporide, the MRM transitions used were *m/z* 321.2 to *m/z* 262.1 and *m/z* 322.1 to *m/z* 263.1, respectively. A proprietary Pfizer compound was used as internal standard, transitions for which were *m/z* 364.3 to *m/z* 228.2. The dwell time of each MRM transition is 50 ms.

Response Correction and Data Processing for Pharmacokinetic Parameters. Data were processed using Applied Biosystems/MDS SCIEX Analyst software, Excel, and Watson LIMS (version 7.2; Thermo Fisher Scientific, Waltham, MA). Analyte peaks were integrated using Analyst 1.4.2 for quantitation and then exported to Excel for response correction. Because the difference between the proto and deutero isotopomers is 1 atomic mass unit, a correction for the deutero compound was necessary because of the contribution from the ^{13}C natural abundance in the proto compound. The response correction factor was calculated from the proto standards in the linear range of the instrument response; the sample response of the deuterated compound was then corrected by subtracting the interference from the proto compound. The response correction factor of deuteron zoniporide was determined from the proto zoniporide standards in the linear range of the instrument response. The responses for deutero zoniporide were corrected by subtracting the contribution from proto zoniporide. The corrected responses were uploaded to Watson LIMS for linear regression and calculations for sample concentrations and pharmacokinetic parameters.

In Vitro KDIEs. The intramolecular deuterium isotope effects for 1-[^{2}H]phthalazine and 2-[^{2}H]quinoxaline were determined from the ratio of the *m/z* 148 and *m/z* 147 mass spectrometric responses in their 1-phthalazone and 2-quinoxalone products. Intermolecular isotope effects on the rate constants for substrate depletion were determined in cytosol, hepatocytes, S-9, or partially purified human aldehyde oxidase using a 1:1 mixture of the deutero and proto forms of quinoline, carbazeran, and zoniporide at 1.0 μM.

Michaelis-Menten kinetic parameters for quinoline and 2-[^{2}H]quinoline were determined with guinea pig liver cytosolic aldehyde oxidase with eight substrate concentrations of quinoline (spanning $\pm 5 \times K_m$) after the linear dependence on time and protein concentration were established. 2-Quinolone was quantitated by UV absorbance at 250 nm for the peak matched with *m/z* 146. Kinetic parameters were determined from *v* versus [*S*] plots using XL-Fit version 4.0.

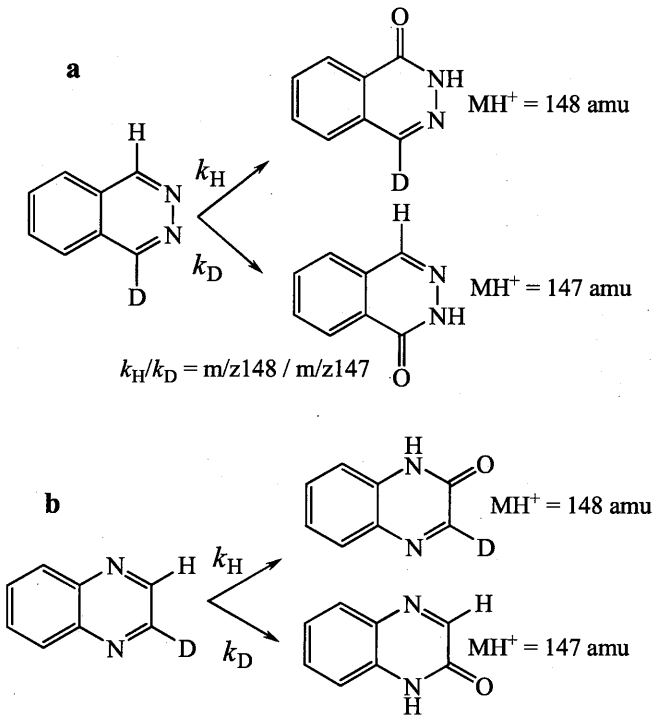

SCHEME 2. Intramolecular deuterium isotope effect determined from the mass spectra of the 2-[^{2}H]quinoxaline and 1-[^{2}H]phthalazine metabolites formed by aldehyde oxidase.

In general, reactions with hepatocytes and S-9 were conducted in a 5-ml volume (0.75×10^6 cells/ml for hepatocytes and 1 mg/ml protein for S-9) in Williams' E medium (hepatocytes) or 50 mM potassium phosphate buffer, pH 7.4 (liver S-9), whereas reactions with liver cytosol or partially purified human aldehyde oxidase were conducted in a 1.0-ml reaction volume in 50 mM potassium phosphate buffer, pH 7.4. Reactions were initiated by addition of substrate to the reaction mixtures that were preincubated at 37°C for approximately 5 min. Over a period of 60 min for cytosol and S-9 reactions and 90 min for hepatocyte reactions, eight 100-μl aliquots were removed and quenched in 100 μl of acetonitrile containing 1% formic acid. A 100-μl aliquot of an internal standard solution (0.5 μM) was added; after mixing, the samples were filtered through a protein-binding filter membrane in a 96-well format. A 25- to 50-μl aliquot was analyzed by MRM of the proto and deutero substrates using substrate-specific transitions. Correction for the peak area of the ^{2}H substrate was done by subtracting the appropriate percentage contribution due to the natural abundance ^{13}C contribution from the ^{1}H substrate. First-order rate constants were determined from the semilogarithmic plots of the ratio of substrate to internal standard versus time. Half-lives were calculated from the equation $t_{1/2} = 0.693$/first-order rate constant. Metabolites were identified by LC-MS from reactions used to determine half-lives in hepatocytes or S-9 supplemented with cofactors or from reactions conducted at 10 μM concentrations of the appropriate substrates.

Kinetic Deuterium Isotope Effects on the Pharmacokinetics of Carbazeran and Zoniporide in Guinea Pig and Rat. All procedures, including dosing methods, are within the guidelines approved by the Pfizer Institutional Animal Care and Use Committee. Male Hartley guinea pigs (325–350 g) and male Sprague-Dawley rats (250–300 g) were used in all pharmacokinetic studies. Carbazeran and zoniporide were dosed as 1:1 mixtures of deutero and proto forms orally (in water) and intravenously as a bolus dose (in saline) via the jugular vein. Carbazeran was dosed at approximately 10 mg/kg b.wt. (5 mg/kg each isotopic form) for both routes of administration, and zoniporide was administered orally at approximately 5 mg/kg b.wt. (2.5 mg/kg each isotopomer) and intravenously at approximately 2 mg/kg b.wt. (1 mg/kg each isotopomer) in saline. Blood samples (0.5 ml) were taken via the carotid artery at appropriate time intervals (between 10 min and 6 h). All samples were kept frozen at −20°C until analysis. Pharmacokinetic parameters were determined only from the experimentally acquired data sets using Watson LIMS.

Results

Synthesis. NMR and mass spectrometric analysis of the deuterated compounds were consistent with their assigned specifically monodeuterated structures as shown in Scheme 1.

In Vitro Kinetic Deuterium Isotope Effects. To establish that interspecies differences observed for metabolism by aldehyde oxidase is not due to species-specific reaction mechanisms, the KDIE was determined for the metabolism of several substrates with liver cytosolic aldehyde oxidase from human, rat, and guinea pig. The isotope effects determined were 1) intramolecular KDIE for 1-[^{2}H]phthalazine and 2-[^{2}H]quinoxaline, 2) intermolecular KDIEs on the first-order rate constants for the oxidations of quinoline/2-[^{2}H]quinoline, carbazeran/1-[^{2}H]carbazeran, and zoniporide/2-[^{2}H]zoniporide; and 3) KDIE on the steady-state kinetic parameters for quinoline and 2-[^{2}H]quinoline with guinea pig liver cytosolic aldehyde oxidase. The aldehyde oxidase-susceptible carbon–hydrogen bonds adjacent to the aromatic nitrogens of phthalazine and quinoxaline are equivalent due to symmetry (Scheme 2). Replacement of either carbon–hydrogen bond by a carbon–deuterium bond provides a direct measure of the intrinsic KDIE from the ratio of the *m/z* 148 and *m/z* 147 ion current intensities in their respective lactam products (Nelson and Trager, 2003). Table 1 shows the results for intra- and intermolecular KDIEs for oxidation of 1-[^{2}H]phthalazine, 2-[^{2}H]and quinoxaline, quinoline/2-[^{2}H]quinoline, carbazeran/1-[^{2}H]carbazeran, and zoniporide/2-[^{2}H]zoniporide by aldehyde oxidase from human, rat, and guinea pig liver. Across species, the intramolecular KDIE was found to be between 4.7 and 5.1 for 1-[^{2}H]phthalazine and 2-[^{2}H]quinoxaline,

TABLE 1

KDIEs for the oxidation of quinoxaline, phthalazine, quinoline, carbazeran, and zoniporide by liver cytosolic aldehyde oxidase from human, rat, and guinea pig, hepatocytes from human and rat, and guinea pig S-9 supplemented with cofactors

Substrate	$^Hk/^Dk$					
	Human		Rat		Guinea Pig	
	Cytosol	Hepatocytes	Cytosol	Hepatocytes	Cytosol	S-9 Supplemented
2-[^{2}H]Quinoxaline[a]	5.0	N.D.[c]	5.1	N.D.	4.7	N.D.
1-[^{2}H]Phthalazine[a]	5.1	N.D.	5.0	N.D.	4.9	N.D.
Quinoline[b]	5.5	N.D.	6.1	N.D.	6.0	N.D.
Carbazeran[b]	4.8	1.5	5.0	4.6	6.0	5.0
Zoniporide[b]	5.8	1.9	3.6	2.7	4.8	1.5

N.D., not determined.

[a] Determined from the ratio of the peak area for *m/z* 148 (^Hk, corrected for the M + 1 contribution from the *m/z* 147 ion) to the *m/z* 147 ion (^Dk).

[b] Determined from the ratio of the rate constants for disappearance of 2-[^{1}H]quinoline (^Hk) and 2-[^{2}H]quinoline (^Dk), 1-[^{1}H]carbazeran (^Hk) and 1-[^{2}H]carbazeran (^Dk), and 2-[^{1}H]zoniporide (^Hk) and 2-[^{2}H]zoniporide (^Dk).

respectively. The intermolecular KDIEs on the first-order rate constants for metabolism of quinoline/2-[^{2}H]quinoline, carbazeran/1-[^{2}H]carbazeran, and zoniporide/2-[^{2}H]zoniporide are between 3.6 and 6.1 across species. The KDIEs on the steady-state kinetic constants for quinoline and 2-[^{2}H]quinoline with guinea pig liver cytosolic aldehyde oxidase show that the KDIE is primarily on V_{max} (5.2) with a small effect on K_m (1.1) resulting in a KDIE of 6.0 on the intrinsic clearance (Table 2). These results are consistent with a common reaction mechanism for aldehyde oxidases from human, rat, and guinea pig liver, where C–H bond cleavage occurs in the rate-limiting step and the KDIE is expressed on the intrinsic clearance in all species.

Metabolically active hepatocytes have the complete complement of drug-metabolizing enzymes and consequently serve as the closest in vitro surrogate for in vivo hepatic metabolism (Fabre et al., 1990). The extent to which aldehyde oxidase contributes to the overall hepatic metabolic transformation of a drug may then be established by examining the KDIE on the intrinsic clearance of the drug in hepatocytes. Guinea pig hepatocytes are not commercially available; therefore, the guinea pig liver S-9 fraction supplemented with NADPH and UDP-glucuronic acid cofactors and alamethicin (to permeate the microsomal membrane) (Fisher et al., 2000) was used to mimic the hepatocyte system as closely as possible (Dalvie et al., 2009). The KDIEs for carbazeran in rat hepatocytes and guinea pig S-9 are 4.6 and 5.0, respectively (Table 1). These values are comparable to the KDIEs with cytosolic aldehyde oxidase of the three species examined (Table 1) and suggest that in the guinea pig and rat aldehyde oxidase is probably the primary route of drug metabolic clearance. In contrast, in human hepatocytes the KDIE is significantly decreased (1.5) (Table 1), suggesting that in humans other metabolic pathways contribute a greater extent of carbazeran's hepatic metabolic clearance. Consistent with this interpretation, the glucuronide of carbazeran was identified as the major metabolite in human hepatocyte reactions with the aldehyde oxidase product secondary (Fig. 1A). Although the carbazeran glucuronide metabolite was also detected in the guinea pig S-9 and rat hepatocyte reactions (Fig. 1, B and C, respectively), the levels were negligible in comparison with that for the aldehyde oxidase metabolite.

The KDIEs for zoniporide with cytosolic aldehyde oxidase from human and guinea pig are similar (5.8 and 4.8) (Table 1). However, with human hepatocytes and guinea pig S-9 supplemented with cofactors, the KDIE is substantially reduced (1.9 and 1.5, respectively) (Table 1). This result suggests that the aldehyde oxidase pathway is not a major metabolic clearance mechanism for zoniporide in the human and guinea pig liver. With rat cytosol the KDIE is somewhat smaller (3.5) (Table 1) than would be expected if aldehyde oxidase were the only enzyme responsible for metabolism and is further decreased in rat hepatocytes (2.7) (Table 1). The decreased KDIE in rat cytosol and hepatocytes is accounted for by other metabolic pathways that are evident from the metabolic profile shown in Fig. 1D for rat hepatocytes. Hydrolysis of the acyl guanidine function to the carboxylic acid (M1) contributes approximately 10%, and other metabolites (M2, M3, M5, M7, M8, and M10) derived from oxidations by cytochromes P450 contribute an additional 40% to the metabolic profile. These pathways account for the decreases in KDIE observed with rat cytosol and hepatocytes and further indicate that the AO pathway contributes approximately 50% of the metabolic clearance in the rat.

Pharmacokinetics of Carbazeran and Zoniporide in the Guinea Pig and Rat Preclinical Models. Pharmacokinetic plots of the log concentration time profiles for carbazeran and 1-[^{2}H]carbazeran administered intravenously or orally to male Hartley guinea pigs and male Sprague-Dawley rats are shown in Fig. 2. The corresponding plots for zoniporide and 2-[^{2}H]zoniporide are shown in Fig. 3. Tabular summaries of the pharmacokinetic parameters for individual animals dosed with carbazeran or zoniporide, either intravenously or orally are given in Tables 3 and 4, respectively. The high clearances of these drugs did not allow for extrapolation to the zero time point for the intravenous route of administration and for oral administration did not adequately define the absorption phase of the pharmacokinetic profiles. Therefore, for both routes of administration, the AUC and $t_{1/2}$ were determined only between the first and last measured time points. The error bars in the log concentration time profiles show that large interanimal variations exist for both drugs by either route of administration. Such variation is commonly observed in pharmacokinetic studies and is compensated for by the use of larger numbers of animals in a study cohort. Cassette dosing of the isotopic forms had two major advantages. First, the KDIE determined on the pharmacokinetic parameters for each animal was obtained under identical physiological conditions, thus eliminating the interanimal variability. Second, animal use was dramatically diminished as the statistical need for large animal cohorts was eliminated. This is evident in the smaller S.D. from the mean for the KDIEs on the pharmacokinetic parameters shown in Table 5.

Intravenous administration of carbazeran in the guinea pig showed a KDIE on the AUC of 5.9 (±0.7). This is comparable to the in vitro KDIE on the intrinsic clearance by guinea pig liver cytosolic aldehyde oxidase and cofactor-supplemented S-9 (6.0 and 5.0, respectively) (Table 1). The systemic elimination half-life showed a small inverse KDIE of 0.8 (±0.1). In contrast, intravenous administration of carbazeran in the rat showed a KDIE of 2.2 (±0.6) on the AUC. This is substantially smaller than the KDIE on the in vitro intrinsic clearance in either rat cytosol or hepatocytes (5.0 and 4.6, respectively) (Table 1). In addition, there is essentially no KDIE on the systemic half-life (1.2 ± 0.2).

Oral administration of carbazeran to male guinea pigs results in KDIEs of 21.4 (±4.3) on the AUC and 22.5 (±7.6) on C_{max}, without a prolongation of systemic half-life. This increase in the isotope effect on the AUC is 3.6-fold higher than the KDIE for intravenously administered carbazeran, suggesting that in the guinea pig oral (intestinal plus hepatic) first-pass metabolism via AO contributes substantially to the clearance of carbazeran. On the basis of the mean AUC for each group, oral bioavailability ($AUC_{p.o.}/AUC_{i.v.} \times 100\%$) for the proto and deuterated forms was 12 and 47%, respectively. The inverse KDIE on the systemic half-life (0.5 ± 0.1) is substantially greater than that observed in the intravenously administered route. In contrast, orally dosed carbazeran in the rat shows a KDIE on the AUC of 2.3 (±0.2), which is comparable to that observed in the intravenous

TABLE 2

KDIE on the steady-state kinetic parameters for the oxidation of 2-[^{2}H]quinoline by guinea pig cytosolic aldehyde oxidase

Substrate	K_m	$^HK_m/^DK_m$	V_{max}	$^HV_{max}/^DV_{max}$	K_m/V_{max}	$^H(K_m/V_{max})/^D(K_m/V_{max})$
	μM		$pmol \cdot min^{-1} \cdot ml^{-1}$			
Quinoline	212		246		1.2	
2-[^{2}H]Quinoline	193	1.1	47	5.2	0.2	6.0

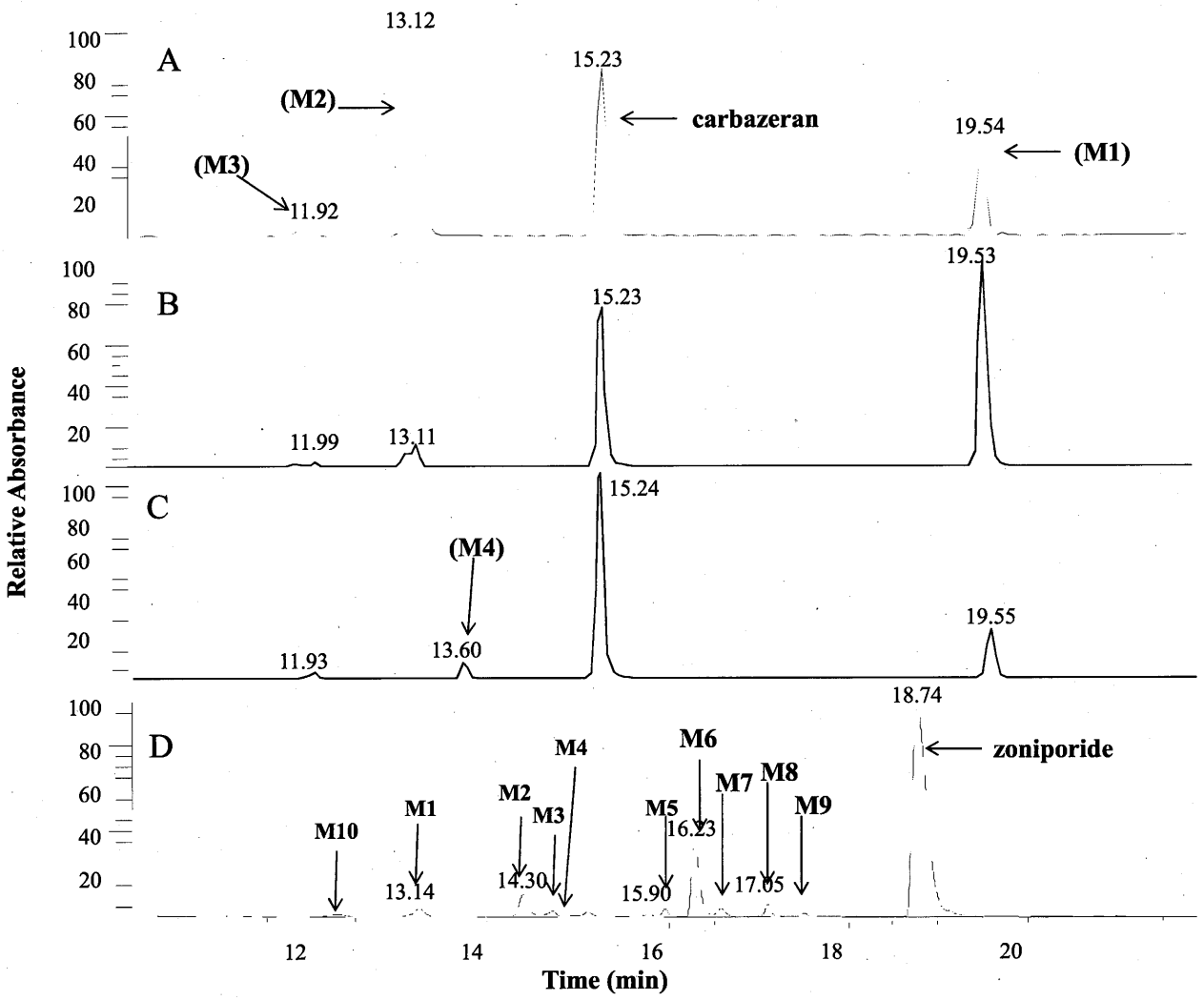

FIG. 1. UV chromatograms (300 nm) of the reaction of carbazeran with hepatocytes or S-9 (supplemented with cofactors) from human (A), guinea pig (B), and rat (C). M1 is the aldehyde oxidase product, M2 is the glucuronide conjugate of carbazeran, and M3 and M4 are the O-decarbamylated and O-demethylated metabolites of carbazeran, respectively. D, UV chromatogram (220 nm) of the zoniporide reaction with rat hepatocytes showing 10 metabolites characterized by MS^n. M6 is the aldehyde oxidase-derived metabolite; M1 is the acyl guanidine hydrolysis product, M2, M3, M5, M7, M8, and M10 are primary cytochrome P450 oxidation products, and M4 and M9 are secondary oxidation products that include oxidation by aldehyde oxidase.

route of administration, suggesting that in the rat oral administration led to the same combination of clearance processes as that after intravenous administration. Based on group mean AUCs, systemic exposure for both the proto and deuterated forms was approximately 3-fold higher after oral administration than with intravenous dosing. Differences in KDIEs on the pharmacokinetic parameters show that guinea pig and rat have substantially different presystemic and systemic clearance mechanisms that affect the pharmacokinetic outcome.

Zoniporide shows no significant KDIE on the pharmacokinetic parameters when dosed either intravenously or orally in the guinea pig. This result is in keeping with the small in vitro KDIE of 1.5 observed on the intrinsic clearance measured in guinea pig liver S-9 supplemented with the cofactors NADPH and UDP-glucuronic acid (Table 1). In the rat, in which in vitro intrinsic clearance shows a KDIE of 3.6 in cytosol and 2.7 in hepatocytes (Table 1), in vivo there is essentially no KDIE on the pharmacokinetic parameters when the drug is dosed intravenously (Table 5). When dosed orally, there appeared to be a small but inverse KDIE on the AUC (0.6 ± 0.2) and C_{max} (0.7 ± 0.1) (Table 5). Thus, despite a small KDIE observed in rat hepatocytes for metabolism of zoniporide, metabolic clearance by aldehyde oxidase does not significantly influence the systemic clearance mechanism in the rat.

Discussion

Mammalian aldehyde oxidases are members of the larger molybdopterin flavoprotein class of enzymes (Garattini et al., 2008). On the basis of immunohistochemical localization in the rat and human, AO-containing cells are ubiquitously distributed to many tissues, with different levels of expression in these tissues between human and rat (Moriwaki et al., 1996, 2001). Species differences in metabolism of various drugs have also been reported for this enzyme (Beedham et al., 1987, 1995; Kawashima et al., 1999; Schofield et al., 2000; Kitamura et al., 2006; Sahi et al., 2008; Magee et al., 2009; Zhang et al., 2011). However, it is unclear whether the enzyme from different species functions by a common reaction mechanism. The aldehyde oxidase-catalyzed oxidation of nitrogen heterocycles has been proposed to involve a nucleophilic addition of molybdopterin-bound hydroxide to the carbon alpha to the heterocyclic nitrogen to give a tetrahedral transition state structure from which either hydride transfer or a proton loss and electron transfer to the molybdopterin cofactor

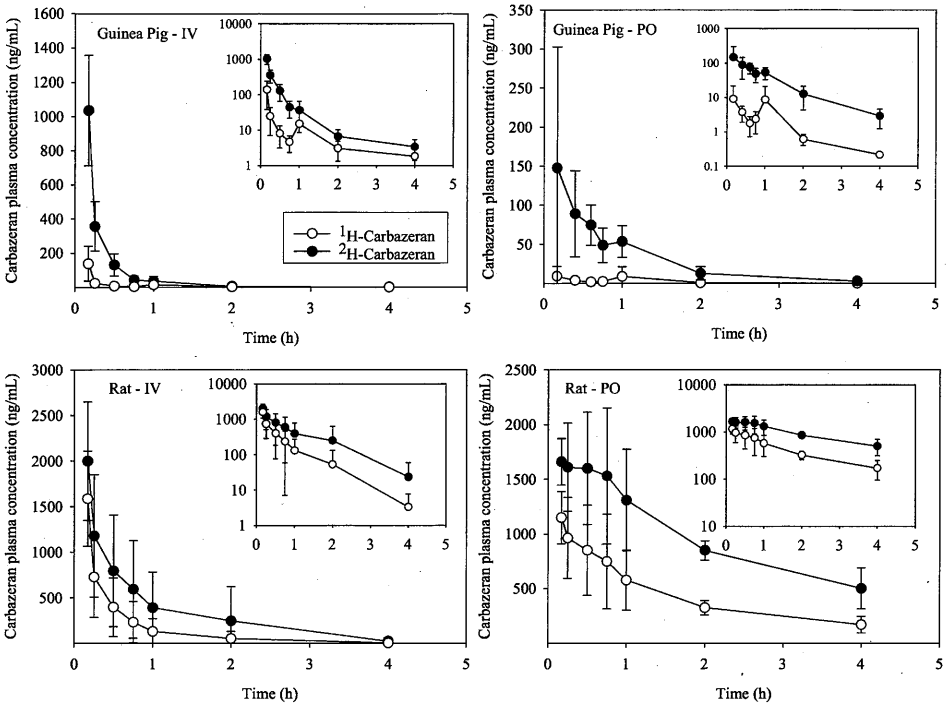

FIG. 2. Plasma concentration versus time profiles for cassette-dosed [^{1}H]carbazeran (○) and [^{2}H] carbazeran (●). Pharmacokinetic profiles are shown for intravenous (top left) or oral (top right) dosing of guinea pigs and for intravenous (bottom left) and oral (bottom right) dosing of rats. The main graphs represent plasma concentration data on a linear scale; insets show the same data on a log-linear scale.

occurs in the rate-limiting step (Xia et al., 1999; Alfaro and Jones 2008). The intra- and intermolecular KDIEs established for quinoxaline, phthalazine, quinoline, carbazeran, and zoniporide establish carbon–hydrogen bond cleavage as the common rate-limiting step for the enzyme across the three species examined in this study, with the magnitude of the effect fully expressed on their intrinsic clearances. Thus, species differences noted for the metabolism of various drugs by aldehyde oxidase must be related either to differences in substrate specificity or enzyme levels rather than the enzyme's reaction mechanism.

Systemic clearance (CL) of any drug after intravenous administration is inversely related to drug exposure over time (AUC) by eq. 1:

$$CL = Dose/AUC \quad (1)$$

CL of any drug is a sum of multiple clearance compartments and is given by eq. 2:

$$CL = CL_H + CL_R + CL_{other} \quad (2)$$

where CL_H and CL_R represent hepatic and renal clearances that are generally major clearance organs and CL_{other} represents clearance

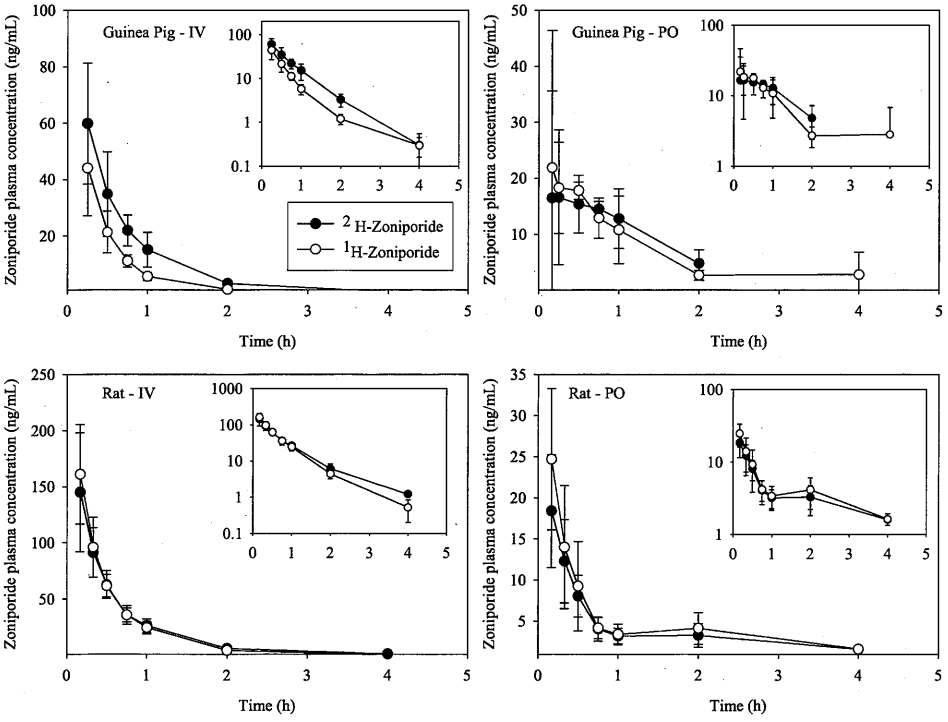

FIG. 3. Plasma concentration versus time profiles for cassette-dosed [^{1}H]zoniporide (○) and [^{2}H]zoniporide (●). Pharmacokinetic profiles are shown for intravenous (top left) or oral (top right) dosing of guinea pigs and for intravenous (bottom left) and oral (bottom right) of rats. The main graphs represent plasma concentration data on a linear scale, insets show the same data on a log-linear scale.

TABLE 3

Pharmacokinetic parameters for intravenously cassette-dosed proto- and deutero-carbazeran and zoniporide to male Hartley guinea pigs and Sprague-Dawley rats

Species	1-^{1}H-		1-^{2}H-	
	AUC	$t_{1/2}$	AUC	$t_{1/2}$
	ng · h/ml	*h*	*ng · h/ml*	*h*
Carbazeran				
GP 02	47.3	2.1	240	1.6
GP 03	19.8	4.4	120	4.1
GP 04	39.7	2.8	259	2.2
Mean	35.6	3.1	206.3	2.6
S.D.	14.2	1.2	75.4	1.3
Rat 1	150	0.5	231	0.5
Rat 2	1000	0.6	2650	0.8
Rat 3	377	0.4	923	0.4
Mean	509	0.5	1268	0.6
S.D.	440	0.1	1245	0.2
Zoniporide				
GP 1	25.8	0.6	51.1	0.5
GP 2	21.6	0.4	34.6	0.5
GP 3	22.3	0.4	36.3	0.5
Mean	23.2	0.5	40.7	0.5
S.D.	2.3	0.1	9.1	0.0
Rat 4	91.3	0.4	94.6	0.6
Rat 5	72.9	0.4	74.8	0.6
Rat 6	58.9	0.3	62.9	0.4
Mean	74.4	0.4	77.4	0.5
S.D.	16.2	0.0	16.0	0.1

mechanisms that include metabolism by other tissues such as lung and intestine and other nonmetabolic clearance mechanisms such as exhalation or direct intestinal excretion. Hepatic and renal clearances include metabolic clearance and nonmetabolic clearance such as biliary excretion and glomerular filtration, both of which are not expected to involve deuterium isotope effects. The metabolic clearance within any compartment can be described in terms of the compartment's blood flow rate (Q) and its intrinsic clearance (CL_{int}) (eq. 3):

$$CL = Q \cdot f_u \cdot CL_{int}/(Q + f_u \cdot CL_{int}) \quad (3)$$

Figure 4 shows a theoretical relationship between clearance by any compartment and the effect of a KDIE of 7.0 on the intrinsic clearance. If $CL_{int} \gg Q$, clearance is limited by blood flow through the compartment and the KDIE on CL for the compartment tends to unity. If systemic clearance is determined exclusively by this compartment, then no isotope effect is expected on systemic half-life, AUC, or C_{max}. In contrast, because metabolic stability of a drug in a given compartment increases, at the limit where $CL_{int} \ll Q$, clearance is limited by the CL_{int}, and the KDIE on CL_{int} is fully expressed on CL for the compartment. If systemic clearance is dominated by this compartment, an isotope effect is expected on systemic half-life, AUC, and C_{max}.

The low systemic exposures (AUCs) for carbazeran and zoniporide after intravenous administration are due to high clearances, estimated to be >400 ml · min^{-1} · kg^{-1}. These rates are in excess of liver blood flow and suggest that additional tissues contribute to clearance. For each metabolic organ, which for AO would include liver, lung, kidney, and intestine, the contributions to systemic clearance are additive (eq. 2) and the magnitude of the deuterium effect is dependent on the relationship of intrinsic clearance to organ blood flow (Fig. 4) and the potential for alternative metabolic and excretory clearance mechanisms.

The low KDIEs observed for zoniporide in guinea pig S-9 and human hepatocytes predict no gain in pharmacokinetic advantage by deuteration in the guinea pig and human. Consistent with this prediction, no pharmacokinetic effect was observed in the guinea pig, whereas in the rat a moderate KDIE is observed with rat hepatocytes and hence a KDIE would be predicted on the pharmacokinetic parameters. The lack of an isotope effect suggests either blood flow-limited AO clearance and/or alternative clearance mechanisms that do not involve an isotope effect. The in vivo disposition of zoniporide in the rat (Dalvie et al., 2010) is consistent with alternate clearance mechanisms in the rat. After an intravenous dose of radiolabeled drug, a total of 87% was recovered in urine and feces; 35% was recovered as the AO-mediated metabolite, 12.3% as non-AO metabolites, and 40% as unchanged zoniporide in feces. Therefore, biliary excretion of unchanged drug represented a substantial component of the systemic clearance.

In the guinea pig, carbazeran shows a KDIE of 5.9 on the AUC after intravenous administration, without a prolongation of half-life. In our experimental protocol, compounds were administered via the jugular vein, and blood samples were withdrawn via the carotid artery, resulting in first-pass exposure to the lung (and heart). Where the dosing and sampling sites differ, the systemic exposure also depends on any degradation in route to the sampling site and eq. 1 becomes (eq. 4)

$$AUC = Fx \times Dose/CL \quad (4)$$

where Fx represents the fraction surviving degradation through tissue x, is less than 1, and differs between the proto and deutero forms due to first-pass metabolism by AO, in this case, the lung.

After oral administration, high clearance compounds due to AO metabolism could still show an isotope effect due to differential first-pass rates based on differing intrinsic clearances. Systemic exposure would be equal to (eq. 5)

$$AUC = Dose/CL \times Fa \times Fg \times Fh \times Fx \quad (5)$$

where Fg and Fh are the fractions surviving passage through the gut wall and first pass through the liver, respectively, and Fx, as above, is the fraction surviving posthepatic elimination en route to the sampling site (carotid artery). With oral administration, the large KDIE on AUC

TABLE 4

Pharmacokinetic parameters for orally cassette-dosed [^{1}H]- and mono-[^{2}H]carbazeran and zoniporide to guinea pigs and Sprague-Dawley rats

Species	1-^{1}H-			1-^{2}H-		
	AUC	C_{max}	$t_{1/2}$	AUC	C_{max}	$t_{1/2}$
	ng · h/ml	*ng/ml*	*h*	*ng · h/ml*	*ng/ml*	*h*
Carbazeran						
GP01	2.54	2.0	0.8	61	65	0.3
GP05	7.09	28.1	1.3	159	377	0.7
GP06	5.89	4.9	0.9	142	102	0.6
GP07	1.48	4.1		22	99	
Mean	4.25	9.8	1.0	96	161	0.5
S.D.	2.67	12.3	0.3	65	145	0.2
Rat 1	2190	1410	1.4	4530	2170	1.7
Rat 2	1350	940	7.0	3240	1430	9.3
Rat 3	1350	1100	1.1	3380	1700	1.4
Mean	1630	1150	3.2	3717	1767	4.0
S.D.	485	239	3.3	708	374	4.0
Zoniporide						
GP 1	17.0	48.4	0.2	20.5	37.4	0.3
GP 2	26.1	14.4	0.6	27.0	15.7	0.6
GP 3	23.6	16.7	0.6	29.7	16.7	0.7
Mean	22.2	26.5	0.5	25.7	23.3	0.5
S.D.	4.70	19.0	0.2	4.73	12.3	0.2
Rat 4	22.6	19.3	0.3	9.3	15.2	0.3
Rat 5	12.9	20.2	0.3	11.1	13.8	0.4
Rat 6	23.6	34.6	0.3	17.8	26.3	0.3
Mean	19.7	24.7	0.3	12.7	18.4	0.3
S.D.	5.9	8.6	0.0	4.0	6.8	0.0

TABLE 5

KDIE on the pharmacokinetic parameters for carbazeran and zoniporide administered intravenously or orally as a cassette dose to male Hartley guinea pigs and male Sprague-Dawley rats

Route	Drug	Species	Mean KDIE (D/H)					
			C_{max}		AUC		$t_{1/2}$	
			Mean	S.D.	Mean	S.D.	Mean	S.D.
Intravenous	Carbazeran	Guinea pig	N.A.	N.A.	5.9	0.7	0.8	0.1
		Rat	N.A.	N.A.	2.2	0.6	1.2	0.2
	Zoniporide	Guinea pig	N.A.	N.A.	1.7	0.2	1.2	0.3
		Rat	N.A.	N.A.	1.0	0.0	1.5	0.3
Oral	Carbazeran	Guinea pig	22.5	7.6	21.4	4.3	0.5	0.1
		Rat	1.5	0.0	2.3	0.2	1.3	0.1
	Zoniporide	Guinea pig	1.0	0.2	1.2	0.1	1.2	0.2
		Rat	0.7	0.1	0.6	0.2	1.1	0.0

N.A., not applicable.

(21.4) (Table 5) observed for carbazeran in the guinea pig suggests a substantial intestinal contribution to first-pass metabolism with blood flow-limited systemic clearance.

In the rat, the higher AUC (lower CL) and a KDIE in hepatocytes of 4.6 would predict an isotope effect in vivo, yet only a modest effect of 2.2 was observed for both routes of administration with no effect on systemic half-life. Because AO appears to be the primary route of metabolism in the rat as is suggested by the KDIE in rat hepatocytes, the low KDIE observed on the AUC with no effect on systemic half-life suggests a clearance approaching the hepatic blood flow limit with no substantial contribution from extrahepatic organs.

In contrast to the guinea pig and rat, the in vitro KDIEs and metabolite profile in human hepatocytes shows that aldehyde oxidase is not the primary metabolic pathway in the human. However, as reported by Kaye et al. (1984), the poor bioavailability of carbazeran in human was attributed to metabolism by aldehyde oxidase. The carbazeran glucuronide was identified as a minor metabolite in urine. This would appear to be in contrast to the metabolites observed in human hepatocytes, in which the carbazeran glucuronide is the dominant metabolite. The carbazeran glucuronide was sensitive to β-glucuronidase (Kaye et al., 1984). This apparent discrepancy between the in vitro and in vivo results can be rationalized by an enterohepatic recycling process, in which the carbazeran glucuronide is excreted via bile and hydrolyzed by intestinal bacteria, and the released carbazeran is reabsorbed, followed by further metabolism by AO and eventual excretion as the AO metabolite. Thus, the magnitude of a KDIE on pharmacokinetic parameters in human would depend on the ultimate extent of elimination via AO versus direct glucuronidation.

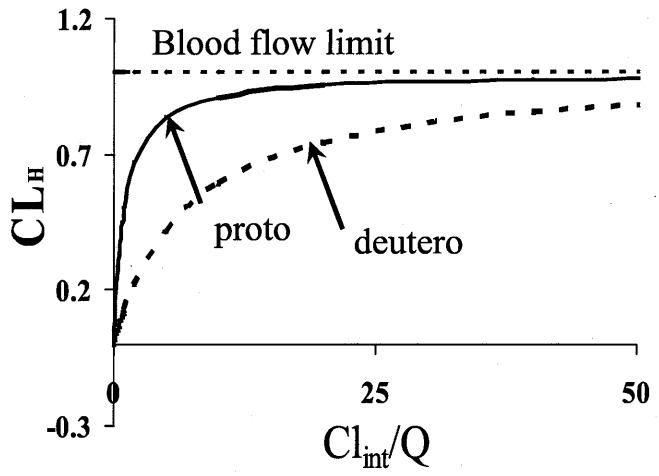

FIG. 4. Theoretical plots showing the relationship of hepatic metabolic clearance with intrinsic metabolic clearance and blood flow (——) and the effect of a KDIE of 7.0 on intrinsic metabolic clearance (– – –) when metabolic clearance is the only clearance mechanism.

The varying impact of isotopic labeling on the pharmacokinetic parameters among different species for two drugs with AO-mediated clearance demonstrates the complexity of the application of KDIEs to pharmacokinetics. From these studies, we conclude that for deuteration as a strategy to alter pharmacokinetics, a clear understanding of the overall clearance rates and mechanisms is critical. When a drug is metabolized by more than one metabolic pathway, it is imperative to know the extent to which each pathway contributes to the overall metabolic clearance, the sites of metabolism, and the mechanisms of the enzymes involved and whether they are expected to show a KDIE on their intrinsic clearances. If the compound possesses low to moderate clearance, deuteration could increase both exposure and half-life. In contrast, for high clearance compounds, deuteration may only reduce the level of first-pass metabolism, thereby increasing systemic exposure but not altering the systemic half-life. Finally, the in vitro approach described herein provides the metabolic basis for the potential use of KDIEs for pharmacokinetic enhancement and can readily rule out use of the strategy but does not assure that pharmacokinetic parameters, such as clearance and oral bioavailability, will be altered.

Authorship Contributions

Participated in research design: Sharma, Gao, and Vaz.

Conducted experiments: Sharma, Strelevitz, Gao, Clark, and Vaz.

Contributed new reagents or analytic tools: Schildknegt.

Performed data analysis: Sharma, Obach, Ripp, Spracklin, Tremaine, and Vaz.

Wrote or contributed to the writing of the manuscript: Tremaine, Ripp, and Vaz.

References

Alfaro JF and Jones JP (2008) Studies on the mechanism of aldehyde oxidase and xanthine oxidase. *J Org Chem* **73:**9469–9472.

Belleau B, Burba J, Pindell M, and Reiffenstein J (1961) Effect of deuterium substitution in sympathomimetic amines on adrenergic responses. *Science* **133:**102–104.

Beedham C, Bruce SE, Critchley DJ, al-Tayib Y, and Rance DJ (1987) Species variation in hepatic aldehyde oxidase activity. *Eur J Drug Metab Pharmacokinet* **12:**307–310.

Beedham C, Critchley DJ, and Rance DJ (1995) Substrate specificity of human liver aldehyde oxidase toward substituted quinazolines and phthalazines: a comparison with hepatic enzyme from guinea pig, rabbit, and baboon. *Arch Biochem Biophys* **319:**481–490.

Bell-Parikh LC and Guengerich FP (1999) Kinetics of cytochrome P450 2E1-catalyzed oxidation of ethanol to acetic acid via acetaldehyde. *J Biol Chem* **274:**23833–23840.

Burm AG, de Boer AG, van Kleef JW, Vermeulen NP, de Leede LG, Spierdijk J, and Breimer DD (1988) Pharmacokinetics of lidocaine and bupivacaine and stable isotope labelled analogues: a study in healthy volunteers. *Biopharm Drug Dispos* **9:**85–95.

Dalvie D, Obach RS, Kang P, Prakash C, Loi CM, Hurst S, Nedderman A, Goulet L, Smith E, Bu HZ, et al. (2009) Assessment of three human in vitro systems in the generation of major human excretory and circulating metabolites. *Chem Res Toxicol* **22:**357–368.

Dalvie D, Zhang C, Chen W, Smolarek T, Obach RS, and Loi CM (2010) Cross-species comparison of the metabolism and excretion of zoniporide: contribution of aldehyde oxidase to interspecies differences. *Drug Metab Dispos* **38:**641–654.

Dunsaed CB, Dornish JM, and Pettersen EO (1995) The bioavailability and dose dependency of the deuterated anti-tumour agent 4,6-benzylidene-d1-D-glucose in mice and rats. *Cancer Chemother Pharmacol* **35:**464–470.

Dyck LE, Juorio AV, Durden DA, and Boulton AA (1988) Effect of chronic deuterated and non-deuterated phenelzine on rat brain monoamines and monoamine oxidase. *Naunyn Schmiedebergs Arch Pharmacol* **337:**279–283.

Fabre G, Combalbert J, Berger Y, and Cano JP (1990) Human hepatocytes as a key in vitro model to improve preclinical drug development. *Eur J Drug Metab Pharmacokinet* **15:**165–171.

Farmer PB, Foster AB, Jarman M, Newell DR, Oddy MR, and Kiburis JH (1979) The metabolism of deuterated analogues of chlorambucil by the rat. *Chem-Biol Interact* **28:**211–224.

Fisher MB, Campanale K, Ackermann BL, VandenBranden M, and Wrighton SA (2000) In vitro glucuronidation using human liver microsomes and the pore-forming peptide alamethicin. *Drug Metab Dispos* **28:**560–566.

Foster AB (1984) Deuterium isotope effects in studies of drug metabolism. *Trends Pharmacol Sci* **5:**524–527.

Garattini E, Fratelli M, and Terao M (2008) Mammalian aldehyde oxidases: genetics, evolution and biochemistry. *Cell Mol Life Sci* **65:**1019–1048.

Hall LR and Hanzlik RP (1990) Kinetic deuterium isotope effects on the N-demethylation of tertiary amides by cytochrome P-450. *J Biol Chem* **265:**12349–12355.

Kawashima K, Hosoi K, Naruke T, Shiba T, Kitamura M, and Watabe T (1999) Aldehyde oxidase-dependent marked species difference in hepatic metabolism of the sedative-hypnotic, zaleplon, between monkeys and rats. *Drug Metab Dispos* **27:**422–428.

Kawazoe Y and Onishi M (1967) Studies on hydrogen exchange. V. Electrophilic deuteration of quinoline and its 1-oxide. *Chem Pharm Bull (Tokyo)* **15:**826–832.

Kaye B, Offerman JL, Reid JL, Elliott HL, and Hillis WS (1984) A species difference in the presystemic metabolism of carbazeran in dog and man. *Xenobiotica* **14:**935–945.

Kitamura S, Sugihara K, and Ohta S (2006) Drug-metabolizing ability of molybdenum hydroxylases. *Drug Metab Pharmacokinet* **21:**83–98.

Kushner DJ, Baker A, and Dunstall TG (1999) Pharmacological uses and perspectives of heavy water and deuterated compounds. *Can J Physiol Pharmacol* **77:**79–88.

Ling KH and Hanzlik RP (1989) Deuterium isotope effects on toluene metabolism. Product release as a rate-limiting step in cytochrome P-450 catalysis. *Biochem Biophys Res Commun* **160:**844–849.

Magee TV, Ripp SL, Li B, Buzon RA, Chupak L, Dougherty TJ, Finegan SM, Girard D, Hagen AE, Falcone MJ, et al. (2009) Discovery of azetidinyl ketolides for the treatment of susceptible and multidrug resistant community-acquired respiratory tract infections. *J Med Chem* **52:**7446–7457.

Moriwaki Y, Yamamoto T, Takahashi S, Tsutsumi Z, and Hada T (2001) Widespread cellular distribution of aldehyde oxidase in human tissues found by immunohistochemistry staining. *Histol Histopathol* **16:**745–753.

Moriwaki Y, Yamamoto T, Yamaguchi K, Takahashi S, and Higashino K (1996) Immunohistochemical localization of aldehyde and xanthine oxidase in rat tissues using polyclonal antibodies. *Histochem Cell Biol* **105:**71–79.

Miwa GT and Lu AY (1987) Kinetic isotope effects and 'metabolic switching' in cytochrome P450-catalyzed reactions. *BioEssays* **7:**215–219.

Najjar SE, Blake MI, Benoit PA, and Lu MC (1978) Effects of deuteration on locomotor activity of amphetamine. *J Med Chem* **21:**555–558.

Nelson SD and Trager WF (2003) The use of deuterium isotope effects to probe the active site properties, mechanism of cytochrome P450-catalyzed reactions, and mechanisms of metabolically dependent toxicity. *Drug Metab Dispos* **31:**1481–1498.

Pryde DC, Dalvie D, Hu Q, Jones P, Obach RS, and Tran TD (2010) Aldehyde oxidase: an enzyme of emerging importance in drug discovery. *J Med Chem* **53:**8441–8460.

Pohl LR and Gillette JR (1984–1985) Determination of toxic pathways of metabolism by deuterium substitution. *Drug Metab Rev* **15:**1335–1351.

Rylander PN (1985) *Best Synthetic Methods: Hydrogenation Methods,* Academic Press, London, UK.

Sahi J, Khan KK, and Black CB (2008) Aldehyde oxidase activity and inhibition in hepatocytes and cytosolic fractions from mouse, rat, monkey and human. *Drug Metab Lett* **2:**176–183.

Schofield PC, Robertson IG, and Paxton JW (2000) Inter-species variation in the metabolism and inhibition of *N*-[(2′-dimethylamino)ethyl]acridine-4-carboxamide (DACA) by aldehyde oxidase. *Biochem Pharmacol* **59:**161–165.

Schneider F, Hillgenberg M, Koytchev R, and Alken RG (2006) Enhanced plasma concentration by selective deuteration of rofecoxib in rats. *Arzneimittelforschung* **56:**295–300.

Schneider F, Mattern-Dogru E, Hillgenberg M, and Alken RG (2007) Changed phosphodiesterase selectivity and enhanced in vitro efficacy by selective deuteration of sildenafil. *Arzneimittelforschung* **57:**293–298.

Tanabe M, Tagg J, Yasuda D, LeValley SE, and Mitoma C (1970) Pharmacologic and metabolic studies with deuterated zoxazolamine. *J Med Chem* **13:**30–32.

Taylor IW, Ioannides C, Sacra P, Turner JC, and Parke DV (1983) Effect of deuteration of imipramine on its pharmacokinetic properties in the rat. *Biochem Pharmacol* **32:**641–647.

Threadgill MD, Baillie TA, Farmer PB, Gescher A, Kestell P, Pearson PG (1989) Primary deuterium kinetic isotope effects on the metabolism and toxicity of *N*-methylformamide in mice, in *Proceedings of the International Symposium on Synthetic Applications of Isotopically Labelled Compounds*; 1988; pp 349–354.

Xia M, Dempski R, and Hille R (1999) The reductive half-reaction of xanthine oxidase. Reaction with aldehyde substrates and identification of the catalytically labile oxygen. *J Biol Chem* **274:**3323–3330.

Zhang X, Liu HH, Weller P, Zheng M, Tao W, Wang J, Liao G, Monshouwer M, and Peltz G (2011) In silico and in vitro pharmacogenetics: aldehyde oxidase rapidly metabolizes a p38 kinase inhibitor. *Pharmacogenomics J* **11:**15–24.

Address correspondence to: Dr. Alfin D. N. Vaz, Department of Pharmacokinetics Dynamics and Metabolism, Pfizer Global Research and Development, Eastern Point Rd., Groton, CT 06340. E-mail: alfin.vaz@pfizer.com